

DOI 10.2478/v10009-007-0033-2  
**Original research paper**

Received: February 22, 2007  
Accepted: September 05, 2007

## Seasonal variability of hydrodynamics in the Vistula Estuary in 1994

Małgorzata Robakiewicz<sup>1</sup>

*Institute of Hydro-Engineering of the Polish Academy of Sciences  
ul. Kościarska 7, 80-328 Gdańsk, Poland*

**Key words:** Vistula Estuary, hydrodynamics, modelling

### Abstract

The Vistula Estuary is a coastal water body boasting free connection with the open sea, where mixing processes of marine and fluvial waters are maintained by local conditions. Based on results from a hydrodynamic model, applied to represent conditions in the year 1994, and using salinity as a tracer, it was found that fluvial water has a tendency to spread westward from the river mouth. This is in contradiction with the dominant wind direction in the region. Model results confirmed field observations of specific hydrological and meteorological conditions required to transport fluvial water northward, towards the Hel Peninsula.

---

<sup>1</sup> E-mail: [marob@ibwpan.gda.pl](mailto:marob@ibwpan.gda.pl)

## INTRODUCTION

Continuous and simultaneous *in situ* measurements of salinity, temperature and currents in the Vistula Estuary have not been carried out to date. At present the only data available comprise long-term systematic observations of hydrological and meteorological conditions at coastal stations, and non-systematic *in situ* measurements in the southern part of the Gulf of Gdańsk.

At the present time the only way of obtaining the data necessary for detailed analyses of time-varying hydrodynamics is re-analysis using a modelling approach. Such an analysis, presented here, was carried out using data for 1994 originating from the 3D hydrodynamic model of the Gulf of Gdańsk, based on Delft3D-FLOW software (license WL|Delft Hydraulics). The subsequent discussion focuses on the model results, with relation to the hydro- and meteorological conditions recorded by the Institute of Meteorology and Water Management (IMGW) in 1994. Special attention is paid to the spreading of fluvial water in the marine environment, and its relationship to hydrological, meteorological and hydrodynamic conditions. This is of interest both scientifically and in that it affords a better understanding of the transport of dissolved pollutants discharged into the Gulf of Gdańsk.

## THE GOVERNING EQUATIONS AND BOUNDARY CONDITIONS OF DELFT3D-FLOW

The Gulf of Gdańsk model was set-up based on Delft3D, the integrated flow and transport system of WL|Delft Hydraulics for the aquatic environment. In this instance the hydrodynamic module Delft3D-FLOW (WL|Delft Hydraulics, 2006) simulates three-dimensional unsteady flow and transport phenomena resulting from meteorological forcing, including the effects of density differences due to non-uniform temperature and salinity distribution. The system solves unsteady shallow water equations in three dimensions. The system of equations consists of horizontal equations of motion, the continuity equation, and transport equations for conservative constituents. The equations are formulated in orthogonal curvilinear coordinates in a horizontal, and  $\sigma$  coordinates in a vertical direction.

The  $\sigma$  coordinate system introduced by Phillips (1957) is defined as:

$$\sigma = \frac{z - \zeta}{d + \zeta} = \frac{z - \zeta}{H}, \quad (1)$$

where:  $z$  – vertical coordinate in physical space;  $\zeta$  – the surface elevation

above the reference plane (at  $z = 0$ );  $d$  – depth below the reference plane;  $H$  – total water depth ( $H = d + \zeta$ ).

Equations written in the transformed system of coordinates are presented below.

Depth averaged continuity equation:

$$\frac{\partial \zeta}{\partial t} + \frac{1}{\sqrt{G_{\xi\xi}}\sqrt{G_{\eta\eta}}} \frac{\partial [(d+\zeta)U\sqrt{G_{\eta\eta}}]}{\partial \xi} + \frac{1}{\sqrt{G_{\xi\xi}}\sqrt{G_{\eta\eta}}} \frac{\partial [(d+\zeta)V\sqrt{G_{\xi\xi}}]}{\partial \eta} = Q, \quad (2)$$

with  $Q$  defined as:

$$Q = H \int_{-1}^0 (q_{in} - q_{out}) d\sigma + P - E, \quad (3)$$

where:  $\xi, \eta$  – horizontal curvilinear coordinates;  $\sqrt{G_{\xi\xi}}$ ,  $\sqrt{G_{\eta\eta}}$  – coefficients used to transform curvilinear to rectangular coordinates;  $U, V$  – depth averaged velocity components in  $\xi$  and  $\eta$  directions, respectively;  $P$  – precipitation;  $E$  – evaporation;  $q_{in}$  – local source per unit volume;  $q_{out}$  – local sink per unit volume.

Momentum equations in horizontal directions  $\xi$  and  $\eta$  are expressed as follows:

$$\begin{aligned} & \frac{\partial u}{\partial t} + \frac{u}{\sqrt{G_{\xi\xi}}} \frac{\partial u}{\partial \xi} + \frac{v}{\sqrt{G_{\eta\eta}}} \frac{\partial u}{\partial \eta} + \frac{\omega}{d+\zeta} \frac{\partial u}{\partial \sigma} + \frac{uv}{\sqrt{G_{\xi\xi}}\sqrt{G_{\eta\eta}}} \frac{\partial \sqrt{G_{\xi\xi}}}{\partial \eta} + \\ & - \frac{v^2}{\sqrt{G_{\xi\xi}}\sqrt{G_{\eta\eta}}} \frac{\partial \sqrt{G_{\eta\eta}}}{\partial \xi} - fv = \\ & = -\frac{1}{\rho_0 \sqrt{G_{\xi\xi}}} P_\xi + F_\xi + \frac{1}{(d+\zeta)^2} \frac{\partial}{\partial \sigma} \left( \mathcal{G}_{mol} + \mathcal{G}_{3D} \frac{\partial u}{\partial \sigma} \right) + M_\xi, \end{aligned} \quad (4)$$

$$\begin{aligned} & \frac{\partial v}{\partial t} + \frac{u}{\sqrt{G_{\xi\xi}}} \frac{\partial v}{\partial \xi} + \frac{v}{\sqrt{G_{\eta\eta}}} \frac{\partial v}{\partial \eta} + \frac{\omega}{d+\zeta} \frac{\partial v}{\partial \sigma} + \frac{uv}{\sqrt{G_{\xi\xi}}\sqrt{G_{\eta\eta}}} \frac{\partial \sqrt{G_{\eta\eta}}}{\partial \xi} + \\ & - \frac{u^2}{\sqrt{G_{\xi\xi}}\sqrt{G_{\eta\eta}}} \frac{\partial \sqrt{G_{\xi\xi}}}{\partial \eta} + fu = \\ & = -\frac{1}{\rho_0 \sqrt{G_{\eta\eta}}} P_\eta + F_\eta + \frac{1}{(d+\zeta)^2} \frac{\partial}{\partial \sigma} \left( \mathcal{G}_{mol} + \mathcal{G}_{3D} \frac{\partial v}{\partial \sigma} \right) + M_\eta, \end{aligned} \quad (5)$$

where:  $P_\xi, P_\eta$  – gradients of hydrostatic pressure,  $F'_\xi, F'_\eta$  – turbulent momentum fluxes,  $u, v$  – flow velocity components,  $M_\xi, M_\eta$  – source or sink of momentum, all in  $\xi$  and  $\eta$  directions, respectively;  $\omega$  - velocity in  $\sigma$  direction;  $f$  – the Coriolis force;  $\mathcal{G}_{mol}$  – kinematic viscosity coefficient;  $\mathcal{G}_{3D}$  – part of eddy viscosity due to 3D turbulence.

Vertical velocity  $\omega$  is computed from the continuity equation:

$$\frac{\partial \zeta}{\partial t} + \frac{1}{\sqrt{G_{\xi\xi}}\sqrt{G_{\eta\eta}}} \frac{\partial [(d+\zeta)u\sqrt{G_{\eta\eta}}]}{\partial \xi} + \frac{1}{\sqrt{G_{\xi\xi}}\sqrt{G_{\eta\eta}}} \frac{\partial [(d+\zeta)v\sqrt{G_{\xi\xi}}]}{\partial \eta} + \frac{\partial \omega}{\partial \sigma} = H(q_{in} - q_{out}). \quad (6)$$

Introducing the shallow water assumption, the vertical momentum is reduced to a hydrostatic pressure equation:

$$\frac{\partial P}{\partial \sigma} = -g\rho H. \quad (7)$$

In the case of non-uniform salinity,  $s$ , and temperature,  $t$ , distribution, the local density is related by the equation of state (Eckart 1958):

$$\rho = \frac{P_0}{\lambda + \alpha_0 P_0}, \quad (8)$$

where:

$$\begin{aligned} \lambda &= 1779.5 + 11.25t - 0.0745t^2 - (3.80 + 0.01t)s, \\ \alpha_0 &= 0.6980, \\ P_0 &= 5890 + 38t - 0.375t^2 + 3s. \end{aligned} \quad (9)$$

Horizontal pressure gradients for the non-uniform density case are expressed as:

$$\begin{aligned} \frac{1}{\rho_0 \sqrt{G_{\xi\xi}}} P_\xi &= \frac{g}{\sqrt{G_{\xi\xi}}} \frac{\partial \zeta}{\partial \xi} + g \frac{d+\zeta}{\rho_0 \sqrt{G_{\xi\xi}}} \int_\sigma^0 \left( \frac{\partial \rho}{\partial \xi} + \frac{\partial \rho}{\partial \sigma} \frac{\partial \sigma}{\partial \xi} \right) \partial \sigma, \\ \frac{1}{\rho_0 \sqrt{G_{\eta\eta}}} P_\eta &= \frac{g}{\sqrt{G_{\eta\eta}}} \frac{\partial \zeta}{\partial \eta} + g \frac{d+\zeta}{\rho_0 \sqrt{G_{\eta\eta}}} \int_\sigma^0 \left( \frac{\partial \rho}{\partial \eta} + \frac{\partial \rho}{\partial \sigma} \frac{\partial \sigma}{\partial \eta} \right) \partial \sigma. \end{aligned} \quad (10)$$

The forces,  $F_\xi$  and  $F_\eta$ , in the momentum equations represent imbalanced horizontal Reynold's stresses. The Reynold's stresses are determined using the eddy viscosity concept:

$$\begin{aligned} F_\xi &= \frac{1}{\sqrt{G_{\xi\xi}}} \frac{\partial \tau_{\xi\xi}}{\partial \xi} + \frac{1}{\sqrt{G_{\eta\eta}}} \frac{\partial \tau_{\xi\eta}}{\partial \eta}, \\ F_\eta &= \frac{1}{\sqrt{G_{\xi\xi}}} \frac{\partial \tau_{\eta\xi}}{\partial \xi} + \frac{1}{\sqrt{G_{\eta\eta}}} \frac{\partial \tau_{\eta\eta}}{\partial \eta}. \end{aligned} \quad (11)$$

For small scale flow, when the shear stresses at the closed boundaries must be taken into account, the shear stresses  $\tau_{\xi\xi}, \tau_{\xi\eta}, \tau_{\eta\xi}, \tau_{\eta\eta}$  are determined accordingly:

$$\begin{aligned} \tau_{\xi\xi} &= \frac{2\mathcal{G}_H}{\sqrt{G_{\xi\xi}}} \left( \frac{\partial u}{\partial \xi} + \frac{\partial u}{\partial \sigma} \frac{\partial \sigma}{\partial \xi} \right), \\ \tau_{\xi\eta} = \tau_{\eta\xi} &= \mathcal{G}_H \left\{ \frac{1}{\sqrt{G_{\eta\eta}}} \left( \frac{\partial u}{\partial \eta} + \frac{\partial u}{\partial \sigma} \frac{\partial \sigma}{\partial \eta} \right) + \frac{1}{\sqrt{G_{\xi\xi}}} \left( \frac{\partial v}{\partial \xi} + \frac{\partial v}{\partial \sigma} \frac{\partial \sigma}{\partial \xi} \right) \right\}, \\ \tau_{\eta\eta} &= \frac{2\mathcal{G}_H}{\sqrt{G_{\eta\eta}}} \left( \frac{\partial v}{\partial \eta} + \frac{\partial v}{\partial \sigma} \frac{\partial \sigma}{\partial \eta} \right). \end{aligned} \quad (12)$$

For 3D shallow water flow the stress tensor is anisotropic. The horizontal eddy viscosity coefficient,  $\mathcal{G}_H$ , is much larger than the vertical eddy viscosity. The horizontal viscosity coefficient is assumed to be a superposition of two parts: (1) 2D part -  $\mathcal{G}_{2D}$  (due to 2D-turbulence), associated with the horizontal motion and forcings not resolved by the horizontal grid; (2) 3D part -  $\mathcal{G}_{3D}$  (due to 3D-turbulence), computed following the turbulence close model:

$$\mathcal{G}_H = \mathcal{G}_{2D} + \mathcal{G}_{3D}. \quad (13)$$

The transport equation is formulated as follows:

$$\begin{aligned} \frac{\partial(d+\zeta)c}{\partial t} + \frac{1}{\sqrt{G_{\xi\xi}}\sqrt{G_{\eta\eta}}} \left\{ \frac{\partial[\sqrt{G_{\eta\eta}}(d+\zeta)uc]}{\partial \xi} + \frac{\partial[\sqrt{G_{\xi\xi}}(d+\zeta)vc]}{\partial \eta} \right\} + \frac{\partial \omega c}{\partial \sigma} = \\ \frac{d+\zeta}{\sqrt{G_{\xi\xi}}\sqrt{G_{\eta\eta}}} \left\{ \frac{\partial}{\partial \xi} \left[ \frac{D_H}{\sigma_{c0}} \frac{\sqrt{G_{\eta\eta}}}{\sqrt{G_{\xi\xi}}} \frac{\partial c}{\partial \xi} \right] + \frac{\partial}{\partial \eta} \left[ \frac{D_H}{\sigma_{c0}} \frac{\sqrt{G_{\eta\eta}}}{\sqrt{G_{\xi\xi}}} \frac{\partial c}{\partial \eta} \right] \right\} + \\ + \frac{1}{d+\zeta} \frac{\partial}{\partial \sigma} \left[ \frac{\mathcal{G}_{mol}}{\sigma_{mol}} + D_{3D} \right] \frac{\partial c}{\partial \sigma} + S, \end{aligned} \quad (14)$$

where  $S$  represents the source/sink term per unit area due to discharge/withdrawal of water, and the exchange of heat through the free surface.

In 3D shallow water flow the diffusion tensor is anisotropic; the horizontal eddy diffusivity,  $D_H$ , is much larger than the vertical eddy diffusivity,  $D_V$ . The horizontal diffusion coefficient is a superposition of the three parts: due to 2D turbulence, due to 3D turbulence and due to molecular diffusion:

$$D_H = D_{2D} + D_V = D_{2D} + D_{3D} + \frac{\mathcal{G}_{mol}}{\sigma_{mol}}. \quad (15)$$

To solve the system of equations the following boundary conditions were introduced. Kinematic boundary conditions:

$$\omega|_{\sigma=-1} = 0 \quad \text{and} \quad \omega|_{\sigma=0} = 0. \quad (16)$$

At the bed the boundary conditions for the momentum equations are:

$$\begin{aligned} \left. \frac{v_H}{H} \frac{\partial u}{\partial \sigma} \right|_{\sigma=-1} &= \frac{1}{\rho_0} \tau_{b\xi}, \\ \left. \frac{v_H}{H} \frac{\partial v}{\partial \sigma} \right|_{\sigma=-1} &= \frac{1}{\rho_0} \tau_{b\eta}, \end{aligned} \quad (17)$$

with  $\tau_{b\xi}$  and  $\tau_{b\eta}$  - the components of the bed stress in  $\xi$  - and  $\eta$  - direction respectively.

At the free surface the boundary conditions for the momentum equations are:

$$\begin{aligned} \left. \frac{v_V}{H} \frac{\partial u}{\partial \sigma} \right|_{\sigma=0} &= \frac{1}{\rho_0} |\tau_s| \cos(\theta), \\ \left. \frac{v_H}{H} \frac{\partial v}{\partial \sigma} \right|_{\sigma=0} &= \frac{1}{\rho_0} |\tau_s| \sin(\theta), \end{aligned} \quad (18)$$

where  $\theta$  is the angle between the wind stress vector, and the local direction of the grid-line  $\eta$  is constant. The magnitude of the wind shear-stress is defined as:

$$|\tau_s| = \rho_a C_d U_{10}^2. \quad (19)$$

where  $\rho_a$  - the air density;  $U_{10}$  - the wind speed 10 m above the free surface;  $C_d$  - the wind drag coefficient.

In the Gulf of Gdańsk model, a water level open boundary was introduced:

$$\zeta + \alpha \frac{\partial}{\partial t} \left\{ U \pm 2\sqrt{gH} \right\} = F_\zeta(t), \quad (20)$$

where  $\alpha$  represents the reflection coefficient to dampen the short waves induced at the start of simulation.

Open boundary conditions for the transport equations are described using the step profile:

$$c_k = \begin{cases} c_{surface}, & z_k > z_d, \\ c_{bottom}, & z_k \leq z_d. \end{cases} \quad (21)$$

where  $z_d$  is a coordinate that specifies the position of discontinuity. Vertical boundary conditions for transport equations are taken as:

$$\begin{aligned} \left. \frac{D_V}{H} \frac{\partial c}{\partial \sigma} \right|_{\sigma=0} &= 0, \\ \left. \frac{D_V}{H} \frac{\partial c}{\partial \sigma} \right|_{\sigma=-1} &= 0. \end{aligned} \quad (22)$$

In the Gulf of Gdańsk model, to determine  $\nu_V$  and  $D_V$  the  $k-\varepsilon$  turbulence closer model is applied, where transport equations are solved for both kinetic energy,  $k$ , and energy dissipation,  $\varepsilon$ . The mixing length  $L$  is calculated according to:

$$L = c_D \frac{k\sqrt{k}}{\varepsilon}. \quad (23)$$

In the transport equations the following assumptions are made: (a) the production, buoyancy and dissipation terms are dominant; (b) the horizontal

length scales are larger than the vertical ones. The transport equations for  $k$  and  $\varepsilon$  are coupled by means of the eddy diffusivity,  $D_V$ , and the dissipation terms. The transport equations for  $k$  and  $\varepsilon$  are given by:

$$\begin{aligned} \frac{\partial k}{\partial t} + \frac{u}{\sqrt{G_{\xi\xi}}} \frac{\partial k}{\partial \xi} + \frac{v}{\sqrt{G_{\eta\eta}}} \frac{\partial k}{\partial \eta} + \frac{\omega}{d+\zeta} \frac{\partial k}{\partial \sigma} = \\ \frac{1}{(d+\zeta)^2} \frac{\partial}{\partial \sigma} \left[ \left( \mathcal{G}_{mol} + \frac{\mathcal{G}_{3D}}{\sigma_k} \right) \frac{\partial k}{\partial \sigma} \right] + P_k + B_k - \varepsilon, \end{aligned} \quad (24)$$

$$\begin{aligned} \frac{\partial \varepsilon}{\partial t} + \frac{u}{\sqrt{G_{\xi\xi}}} \frac{\partial \varepsilon}{\partial \xi} + \frac{v}{\sqrt{G_{\eta\eta}}} \frac{\partial \varepsilon}{\partial \eta} + \frac{\omega}{d+\zeta} \frac{\partial \varepsilon}{\partial \sigma} = \\ \frac{1}{(d+\zeta)^2} \frac{\partial}{\partial \sigma} \left[ \left( \mathcal{G}_{mol} + \frac{\mathcal{G}_{3D}}{\sigma_\varepsilon} \right) \frac{\partial \varepsilon}{\partial \sigma} \right] + P_\varepsilon + B_\varepsilon - c_{2\varepsilon} \frac{\varepsilon^2}{k}, \end{aligned} \quad (25)$$

where:

$$P_k = \mathcal{G}_H \frac{1}{(d+\zeta)^2} \left[ \left( \frac{\partial u}{\partial \sigma} \right)^2 + \left( \frac{\partial v}{\partial \sigma} \right)^2 \right], \quad (26)$$

$$B_k = \frac{\mathcal{G}_{3D}}{\rho_0} \frac{g}{H} \frac{\partial p}{\partial \sigma}, \quad (27)$$

$$P_\varepsilon = c_{1\varepsilon} \frac{\varepsilon}{k} P_k, \quad (28)$$

$$B_\varepsilon = c_{1\varepsilon} \frac{\varepsilon}{k} (1 - c_{3\varepsilon}) B_k, \quad (29)$$

with  $c_{1\varepsilon} = 1.44$ ,  $c_{1\varepsilon} = 1.92$ ,  $c_{1\varepsilon} = 1.0$ .

The vertical eddy viscosity  $\mathcal{G}_v$  is determined by:

$$\mathcal{G}_v = c'_\mu L \sqrt{k} = c_\mu \frac{k^2}{\varepsilon}, \quad (30)$$

where  $c'_\mu$  - constant in Kolmogorov-Prandtl's viscosity formulation,  $c_\mu$  - calibration constant:

$$c_{\mu} = c_D c'_{\mu}, \quad (31)$$

where  $c_D$  is a constant determined by calibration

$$c_D = c_{\mu}^{3/4} \approx 0.1925. \quad (32)$$

To solve the system of equations, boundary conditions are specified. For local equilibrium of production and dissipation of kinetic energy it is assumed at the bed that:

$$k|_{\sigma=-1} = \frac{u_{*b}^2}{\sqrt{c_{\mu}}}, \quad (33)$$

and at the free surface:

$$k|_{\sigma=0} = \frac{u_{*s}^2}{\sqrt{c_{\mu}}}, \quad (34)$$

with  $u_{*b}$  - the friction velocity at the bed,  $u_{*s}$  - the friction velocity at the free surface. For the transport equation of the dissipation,  $\varepsilon$ , the following conditions are used at the bed:

$$\varepsilon|_{\sigma=-1} = \frac{u_{*b}^3}{\kappa z_0}, \quad (35)$$

and the surface:

$$\varepsilon|_{\sigma=0} = \frac{u_{*s}^3}{0.5\kappa\Delta z_s}. \quad (36)$$

where  $z_0$  - bed roughness length,  $\Delta z_s$  - thickness of the surface layer.

## HYDROLOGICAL AND METEOROLOGICAL CONDITIONS IN 1994

Hydrodynamics in the Vistula Estuary, located in the southern part of the Gulf of Gdańsk, are mainly driven by local hydrological and meteorological conditions. Therefore, to represent the hydrodynamics of this region in a realistic way a comprehensive knowledge of these forces is essential. Analysis of these conditions for 1994 is presented below.

The average Vistula river discharge in 1994 was  $1040 \text{ m}^3 \text{ s}^{-1}$ , which is reasonably close to the average of 1951–1990 at  $1080 \text{ m}^3 \text{ s}^{-1}$  (Fal et al. 1997). Greater differences are seen between mean monthly values than between the year groups (Table 1). Analysis of river discharge in 1994 indicates that the extreme values reached a max. of  $3930 \text{ m}^3 \text{ s}^{-1}$  and min.  $349 \text{ m}^3 \text{ s}^{-1}$ ; well within the maximal range observed in the years 1951-1990 (max.  $7840 \text{ m}^3 \text{ s}^{-1}$ , min.  $253 \text{ m}^3 \text{ s}^{-1}$ ). Seasonal differences in river discharge in 1994 are illustrated in Fig. 1. The maximal yearly values were encountered in spring, with discharge exceeding  $1000 \text{ m}^3 \text{ s}^{-1}$  for most of that period. In the summer and winter months the discharge hardly ever exceeded  $1000 \text{ m}^3 \text{ s}^{-1}$ , whilst in autumn it did not even reach that value.

**Table 1**

Vistula River discharge, measured at the Tczew station, in the years 1994 and 1951-1990

month	1994			1951-1990		
	$Q_{\text{aver}}$ [ $\text{m}^3 \text{ s}^{-1}$ ]	$Q_{\text{min}}$ [ $\text{m}^3 \text{ s}^{-1}$ ]	$Q_{\text{max}}$ [ $\text{m}^3 \text{ s}^{-1}$ ]	$Q_{\text{aver}}$ [ $\text{m}^3 \text{ s}^{-1}$ ]	$Q_{\text{min}}$ [ $\text{m}^3 \text{ s}^{-1}$ ]	$Q_{\text{max}}$ [ $\text{m}^3 \text{ s}^{-1}$ ]
I	1043	972	1190	1120	302	4250
II	988	565	1450	1520	324	4530
III	1566	892	2410	1870	304	6980
IV	2663	1980	3930	1870	489	7020
V	1224	964	1790	1230	504	4240
VI	1176	732	2080	1040	475	7840
VII	544	433	804	919	335	5050
VIII	392	349	463	887	300	6820
IX	463	397	589	720	300	3390
X	636	499	820	786	306	5500
XI	761	595	964	993	319	4460
XII	1052	772	1760	968	253	3830
I - XII	1040	397	3940	1080	253	7840

The 1994 water temperature variations at the Tczew station on the Vistula River are presented in Table 2. The average that year was  $10.3^\circ\text{C}$ , with a minimum of  $0.6^\circ\text{C}$  and a maximum of  $26.4^\circ\text{C}$ . Unfortunately, comparable, long-term water temperature data are not available.

**Table 2**

The Vistula River temperature, measured at the Tczew station, in 1994

month	$T_{aver}$ [°C]	$T_{min}$ [°C]	$T_{max}$ [°C]
I	1.86	1.6	2.2
II	1.07	0.6	1.8
III	3.15	1.0	6.4
IV	9.15	6.4	14.0
V	15.18	12.4	17.6
VI	17.23	15.6	20.8
VII	23.27	20.8	26.0
VIII	20.96	17.0	26.4
IX	15.07	13.2	17.4
X	8.34	5.2	12.8
XI	4.01	2.4	6.2
XII	3.21	2.2	4.0
I - XII	10.27	0.6	26.4

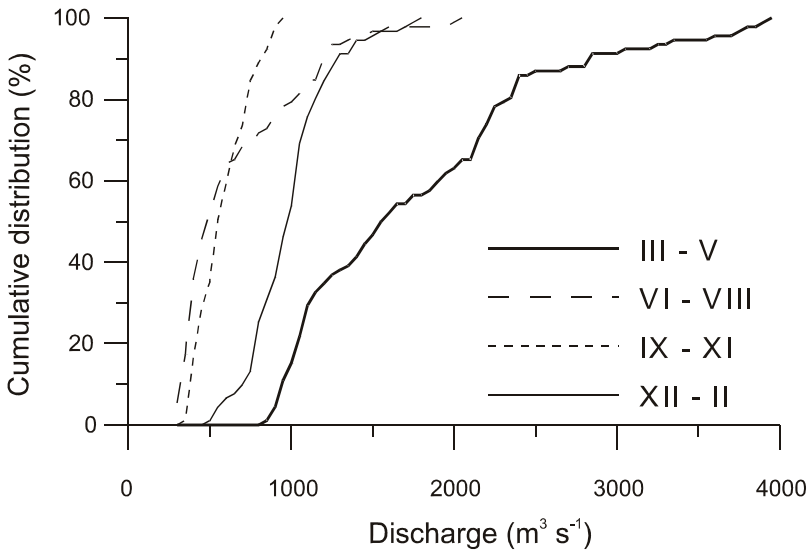


**Fig. 1.** Frequency of seasonal Vistula River discharge rate in 1994.

A comparison between the daily solar radiation, recorded at the Gdynia station, and the water temperature of the Vistula River, at the Tczew station, in

1994 (Fig. 2) shows a rather high correlation between the two ( $R^2 = 0.8352$ ), with a clear time shift between the maxima of both parameters. The maximum water temperature in the river was reached when the river discharge was at its lowest (Fig. 2).

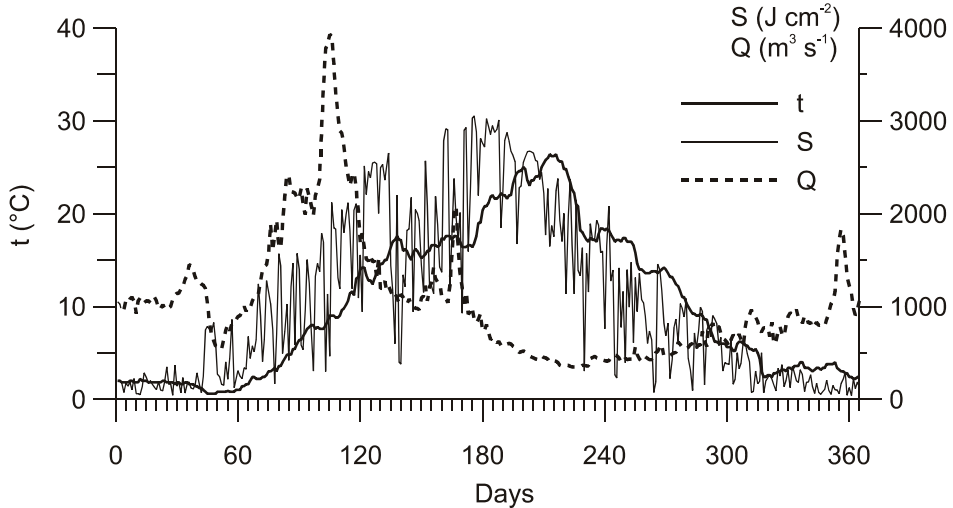


**Fig. 2.** Changes in Vistula River discharge rate (**Q**), water temperature (**t**) at Tczew station, and daily solar radiation (**S**) at Gdynia meteorological station, in 1994.

Wind plays a very important role in the generation of currents in the Gulf of Gdańsk. In that region wind direction and speed are very changeable with time; there is no particular wind direction that can be associated with a given season. A comparison of wind statistics in the years 1994 and 1951-1975 (Kwiecień 1990) for the Hel station is shown in Table 3. In 1994 the frequency of westerly winds (directions W, NW, SW) was higher than in the years 1951-1975, while

**Table 3**

Mean frequency of direction (%) and mean wind speed [ $m\ s^{-1}$ ], measured at Hel station, in the years 1994 and 1951-1975

		N	NE	E	SE	S	SW	W	NW	C
1994	%	7.88	7.60	10.43	9.04	14.65	13.08	23.28	13.15	0.89
	[ $m\ s^{-1}$ ]	2.6	2.7	2.9	3.0	3.3	3.4	4.0	3.3	
1951-1975	%	8.0	8.9	10.2	9.5	13.3	12.1	19.8	12.3	5.9
	[ $m\ s^{-1}$ ]	4.3	4.4	4.2	4.1	4.1	4.7	5.2	4.9	

the frequency of calm weather was lower (only 0.89%) than in the earlier years (5.9%). In comparing the mean annual wind velocities it can be seen that in 1994 wind was generally weaker than in the years 1951-1975. Frequency analysis of seasonal variability of wind speed and direction (Fig. 3) depicts the west wind as the most common and the strongest in all seasons. In general in 1994 north winds were more common than those from the south in spring and summer, while in autumn and winter the opposite situation was the case.

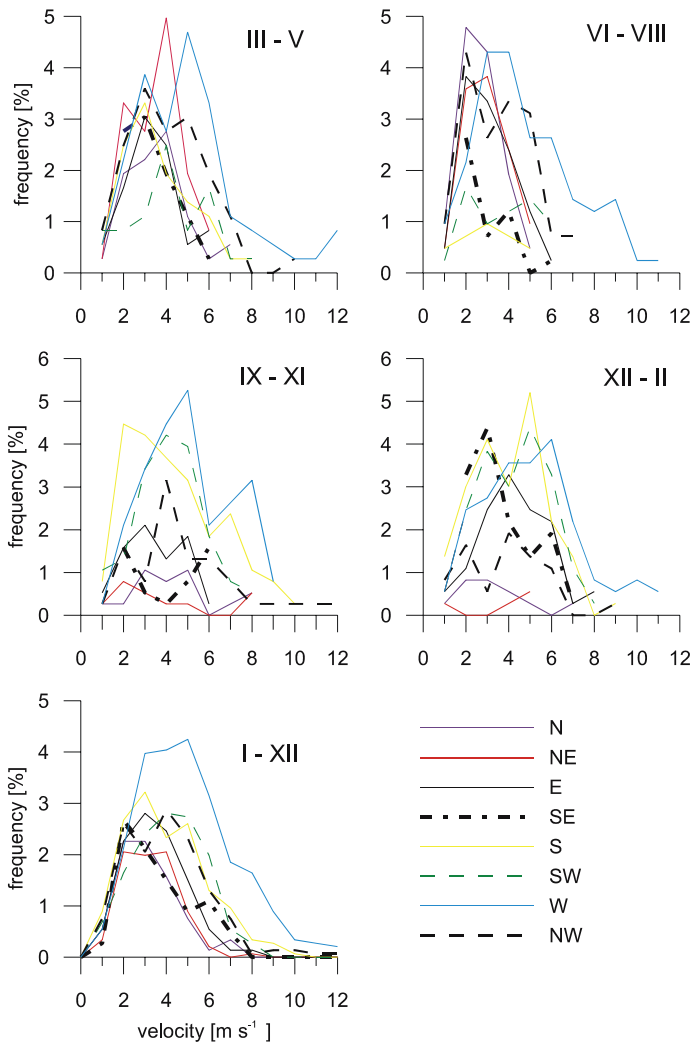


**Fig. 3.** Frequency distribution of seasonal wind speed at Hel station in 1994.

## SALINITY, TEMPERATURE AND WATER CURRENT VARIATIONS

Hydrodynamics of the Gulf of Gdańsk in 1994 were modelled using a 3D set-up based on Delft3D-FLOW as described in Section 2. This took into account all of the major forces in the region (i.e. wind magnitude and direction, water levels, river discharge, river temperature, and solar radiation), based on the IMGW measurements. Table 4 shows the frequencies and locations of the forcing data used. It should be noted that a uniform wind field over the whole area, analogous to that at the Hel station, was applied. Wind varies in both time and space naturally; however, reliable wind measurements are not available for the whole of this region. Only a few stations in the area record wind characteristics; all of them located on the coast. Analysis of wind characteristics carried out by Kwiecień (1990) led to the conclusion that wind measurements recorded at the Hel station can be used as representative for the Gulf of Gdańsk.

**Table 4**

Forcing data applied for representation of hydrodynamics in 1994

<b>forcing</b>	<b>frequency</b>	<b>location of measurement</b>
wind speed and direction	6 hours	Hel station
discharge: Vistula River	1 day	Tczew station
discharge: Pregola and Niemen Rivers	5 days	estimate based on data published by Kwiatkowski et al. (1997)
water temperature: Vistula, Pregola and Niemen Rivers	1 day	Tczew station
solar radiation	1 day	Gdynia station
air temperature	12 hours	Hel station
humidity	1 day	Hel station

Measurements of the inflow of fresh water by the Vistula River were taken from the Tczew station, situated about 30 km upstream from the river mouth, the last station on the Vistula River that is not directly influenced by the Baltic Sea. Lack of direct measurements for the Niemen and Pregola rivers were overcome by estimates based on the literature (Kwiatkowski et al. 1997).

When considering changes of hydrodynamics over the scale of seasons it is crucial to incorporate heat exchange processes. Changes of heat fluxes from the atmosphere were introduced into the model with a time step of 1 hour. These values were estimated using daily solar radiation measurements from the Gdynia station (the only station measuring that parameter in the analysed region), taking into account the day length characteristic for its geographic position.

In order to schematicise the area of the Gulf of Gdańsk model, the curvilinear orthogonal grid in the horizontal and 20 layers using  $\sigma$  coordinates

in a vertical direction were adopted (Robakiewicz 1997). The model was calibrated using POLRODEX'96 experimental data, and verified for the year 1994 (Robakiewicz 1997, 2000, 2004). The analysis concentrates on the identification of fluvial water in the marine environment. The analyses presented are based on results from the upper-most layer of the numerical model, having a thickness of 0.5% of the total depth, which represents a water layer 0.1-0.3 m thick at the locations chosen for comparison. However, it was found that considering a water layer of nearly the same 0.3 m thickness, analogous salinity and temperature values were found in all of the analysed locations.

Water temperature was considered as a marker to trace the spreading of fluvial water in the sea. The surface temperature of fluvial and marine waters were explored (Fig. 4) at sites in the Gulf of Gdańsk (Fig. 5) and the Vistula River, and the frequency distributions plotted (Fig. 6). It was noted that in all seasons, except winter, the temperature differences between locations **A**, **C** and **T** tended to be very small. Comparisons between seasonal water temperatures in the Vistula River and the sites in the Gulf of Gdańsk are shown in Figure 7. In spring and summer, fluvial water was warmer than that of marine origin, while in winter the opposite was true; autumn was an intermediate period with no clear difference. This lack of clear pattern means that water temperature is not a useful indicator of fluvial water dispersion into the sea at all times of year.

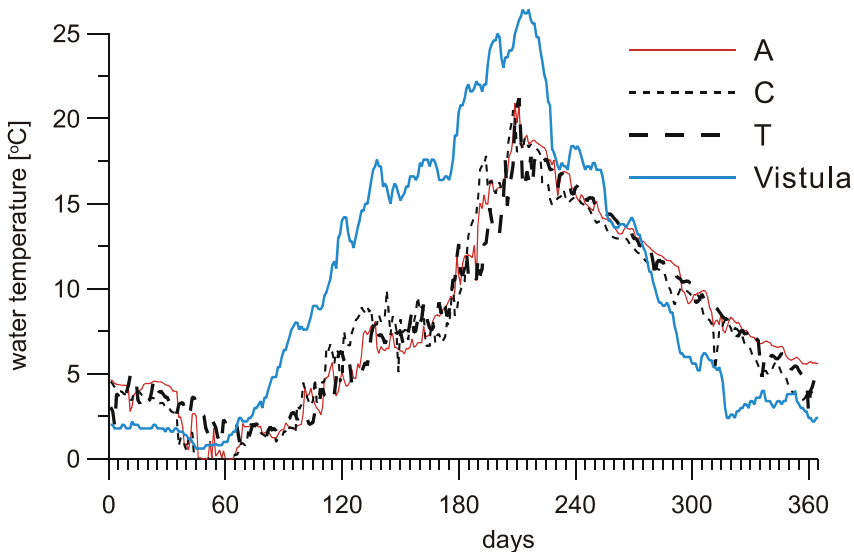


**Fig. 4.** Water surface temperature at locations **A**, **C**, **T** and the Vistula River in 1994.

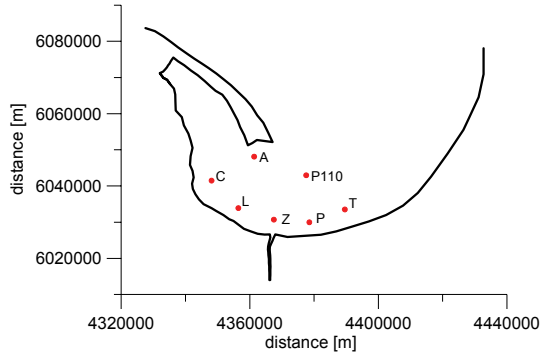


**Fig. 5.** Location of modelled sites in the Gulf of Gdańsk.

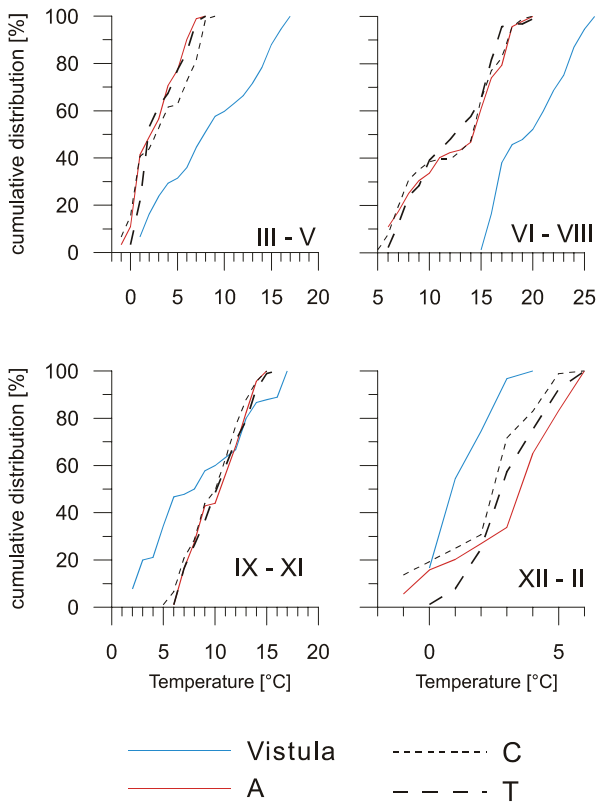


**Fig. 6.** Frequency distribution of seasonal water temperature in the Vistula River and locations A, C and T in 1994.

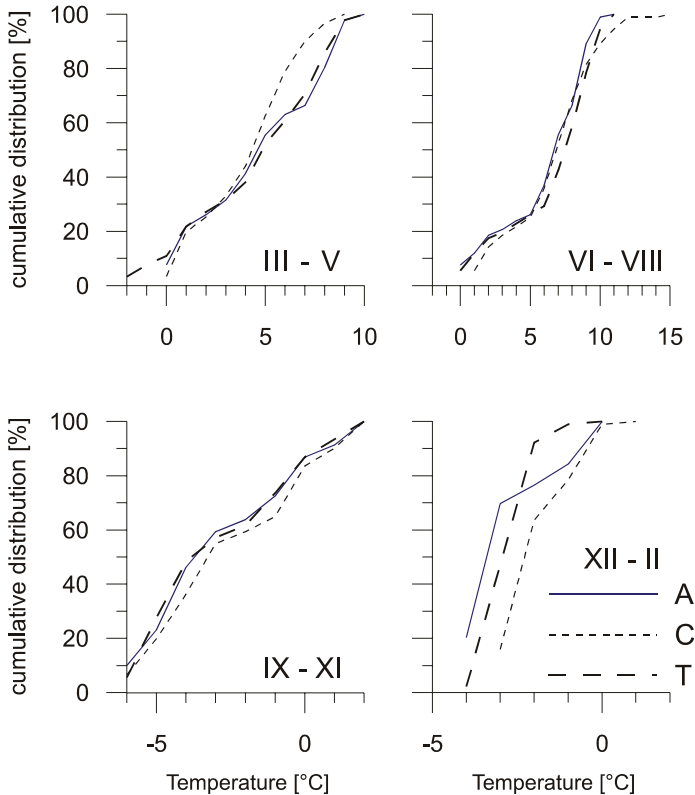


**Fig. 7.** Frequency distribution of seasonal water temperature of fluvial and marine water at locations A, C and T in 1994.

As a result of water temperature being a poor indicator of the extent of fluvial water in the marine environment, salinity differences were analysed for this purpose. To analyse the spatial extent of fluvial waters in the Gulf of Gdańsk some characteristic locations were chosen: **T** and **P** – eastward spreading, **C** and **L** – westward spreading, **A** and **P110** – northward spreading, and **Z** – in the vicinity of the river mouth (see Fig. 5). A relatively large volume of fresh water flows into the Gulf of Gdańsk through the man-made channel, thus effectively placing the river mouth at a distance from the shoreline. In this way the fluvial water maintains its physiochemical properties away from the coast. A boundary between the two water types, marine and fluvial, creates a hydrological front. It has been reported (Nowacki and Matciak 1996, 2000) that the front corresponds to the isohaline 4.5–5.1 PSU. For the purpose of these analyses, the 5 PSU isohaline was taken as the boundary.

Salinity measurements were investigated at locations **A**, **C** and **Z** throughout 1994 (Fig. 8). The results show very varied salinities at the three sites, indicating that the impacts of fluvial water inputs depend not only on the distance from the river mouth, but also on other factors. At the site closest to the river mouth (location **Z**), salinity decreased from time to time below 3 PSU, while at the other locations it rarely dropped below 4 PSU. Visual comparison of the temporal salinity variations at locations **A** and **C**, which are equidistant from the river mouth, showed them to be markedly different.

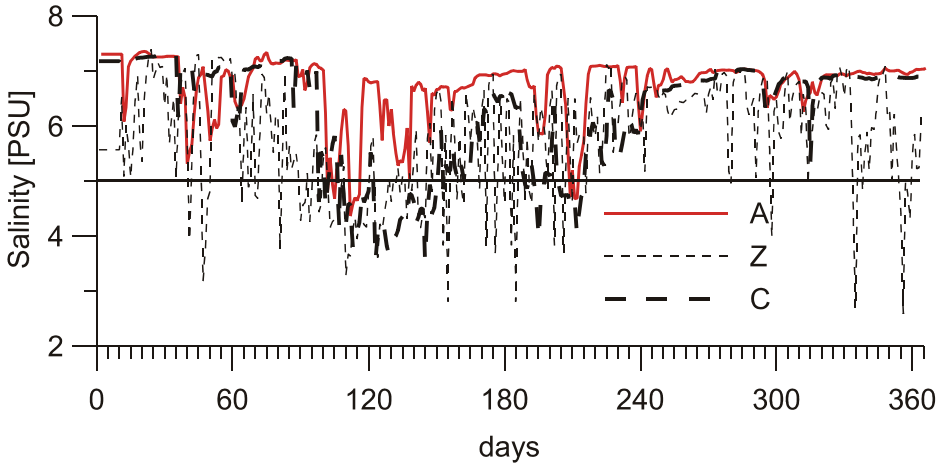


**Fig. 8.** Salinity changes at locations **Z**, **A** and **C** in 1994.

Initial comparisons considered the salinity at the chosen locations over 1994 as a whole. At the site closest to the river mouth - location **Z** - salinity varied within the range 2-7.5 PSU; with salinity below 5 PSU about 26% of the time (Fig. 9). At sites north of the river mouth, i.e. locations **A** and **P110**, the salinity was about 7 PSU much of the time. The frequency of occasions in which the salinity was recorded to be below 5 PSU was similar for locations **A** and **P110**, at only about 3% of the time. This last result corroborates previous reports in the literature (e.g. Majewski and Bogacka 1983) in which low salinity has occasionally been observed in the Hel Peninsula vicinity. In 1994 this situation was observed only three times, each of them lasting not more than a few days (Fig. 8). The collected data enabled comparisons of the frequency of occurrence of fluvial water in the areas located to the east and west of the river mouth. To this end locations **T** and **C**, both about 20 km from **Z**, and **L** and **P** both about 10 km away were chosen. At **T** the frequency of events when salinity was recorded below 5 PSU was approximately 4%, while for **C** it was

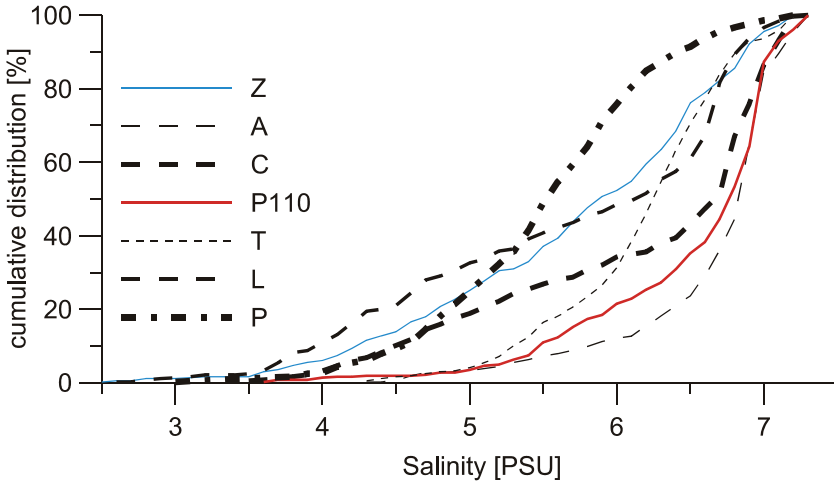


**Fig. 9.** Salinity distribution at chosen locations in the Gulf of Gdańsk in 1994.

about 19%. The frequency of the same events at the locations closer to the river mouth were at **L** about 32%, and 25% at **P** (Fig. 9).

The occasions at which the salinity fell below 5 PSU at locations **A**, **C** and **T** was seen to be seasonally variable, occurring most frequently in spring (Fig. 10). The frequency of salinity <5 PSU was higher at location **C**, about 50% of the time in spring, than at **A** and **T**, about 10% of the time each. In summer these low salinities were also observed, but with much lower frequency

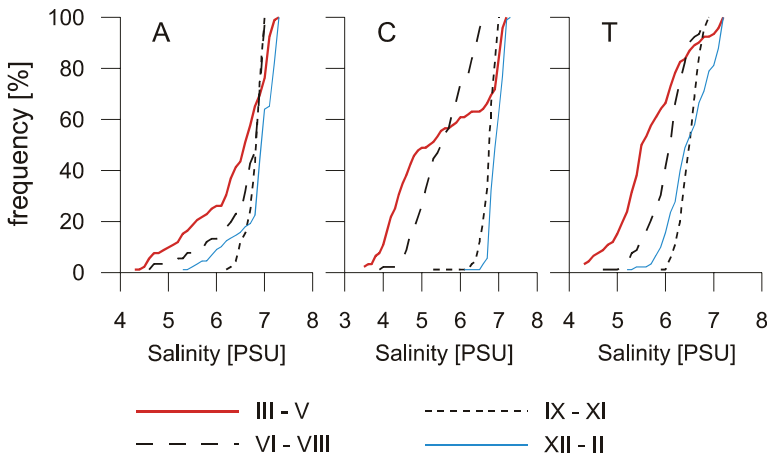


**Fig. 10.** Seasonal salinity distribution at locations **A**, **C** and **T** in 1994.

(location **C** – 25%; locations **A** and **T** – below 4%). In the autumn and winter seasons, salinity was always higher than 5 PSU at all three sites. These results imply that fluvial water had a tendency to spread more westward than eastward in 1994. This result is rather unexpected, since the water flow from the estuary is generally eastward as a consequence of the dominating westerly winds (Tab. 3).

Analysis of seasonal variability in surface current direction (Fig. 11) shows that at location **T** an easterly current generally dominated in 1994 (conforming to the predominant wind direction at Hel station); only in winter did easterly and westerly currents have similar frequencies. At location **A**, in the spring a

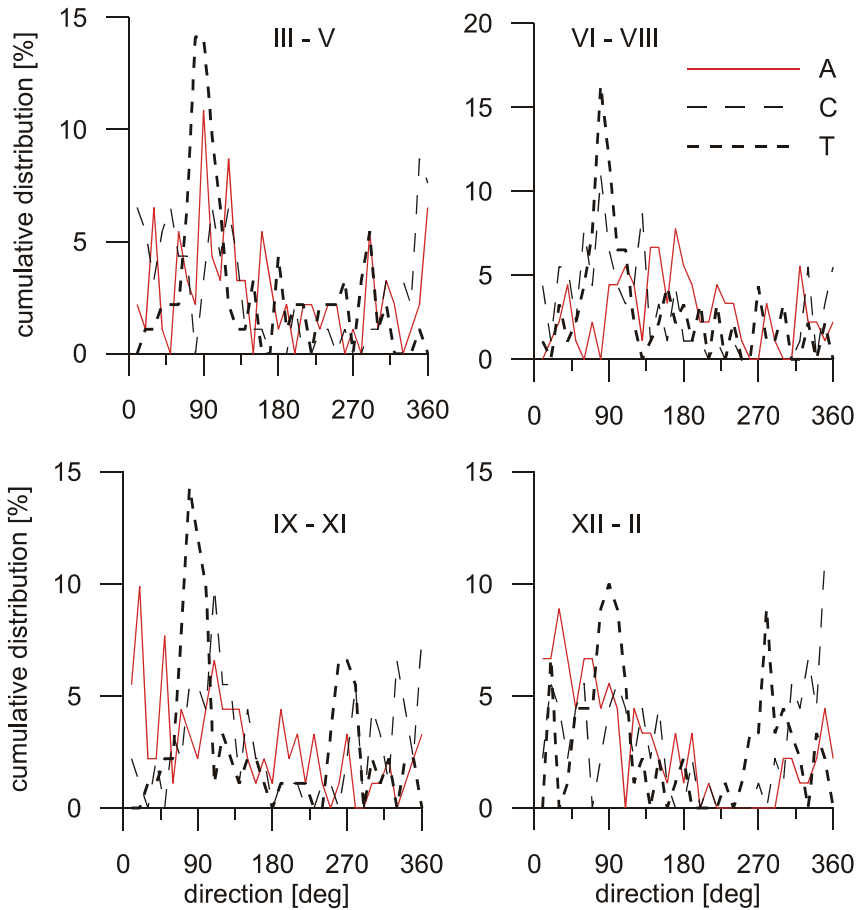


**Fig. 11.** Seasonal distribution of water current direction at locations **A**, **C** and **T** in 1994.

westerly current predominated, while in the autumn and winter southerly directions of flow were most frequent. At location **C** the prevailing direction was not as marked as at location **T**; however, a low frequency of currents directed southward was observed. The current speeds (Fig. 12) were very similar at locations **A** and **C**. The maximum speed reached was  $0.25 \text{ m s}^{-1}$  in the autumn, and  $0.2 \text{ m s}^{-1}$  in the remaining seasons, although most of time (at least 80%) they did not exceed  $0.1 \text{ m s}^{-1}$ . At location **T** the current speeds were higher, with maximum values reaching  $0.5 \text{ m s}^{-1}$  in winter, although the majority (over 80%) were again slower, at below  $0.2 \text{ m s}^{-1}$ . The relatively high current speeds at location **T** are associated with the semi-circular shape of the area, which is partly enclosed by the Hel Peninsula, specific bathymetry and the influence of the rotational motion of the Earth. This water movement explains the low frequency of observations of salinity below 5 PSU at location **T**.

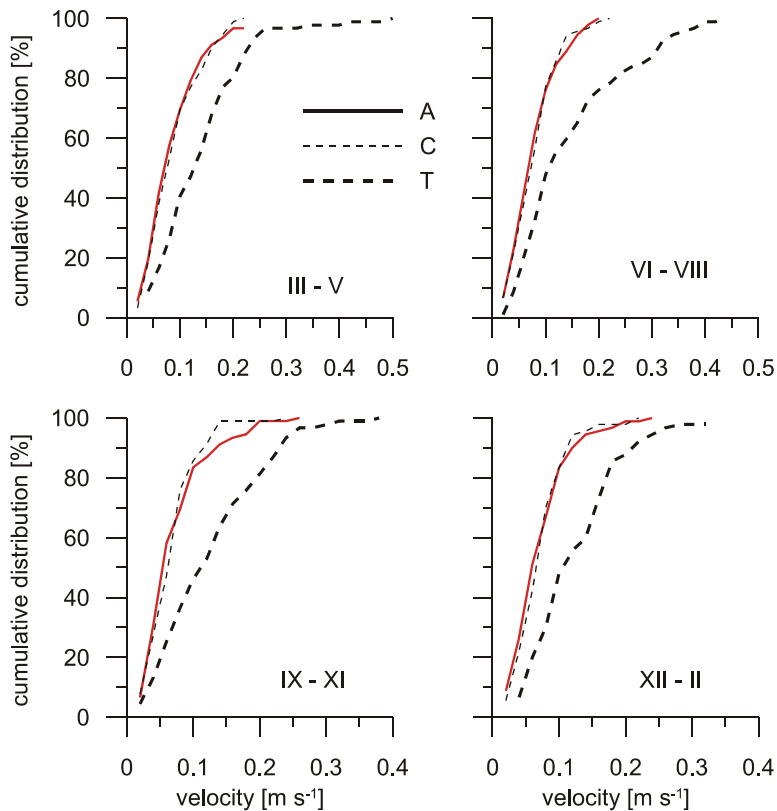


**Fig. 12.** Distribution of velocity magnitude in locations **A**, **C** and **T** in seasons of the year 1994.

From the analyses it can be seen that not only do wind-generated surface currents play an important role in spreading the fluvial water over considerable distances, but the amount of fresh water discharged into the system is also important. This is well illustrated by results at locations **T**, **A** and **C** (Fig. 13) where the relationship between salinity, river discharge, wind direction and wind speed is illustrated. The amount of water that must be discharged into the estuary to enable fluvial water to be traced on the surface depends on the location in the Vistula Estuary. A river discharge of about  $2000 \text{ m}^3 \text{ s}^{-1}$  is needed for this to be detectable at location **A**, whilst about  $1500 \text{ m}^3 \text{ s}^{-1}$  will enable its detection at location **T**. Penetration of fluvial water to the western part of the Estuary (location **C**) is evident even in cases of relatively low discharges.

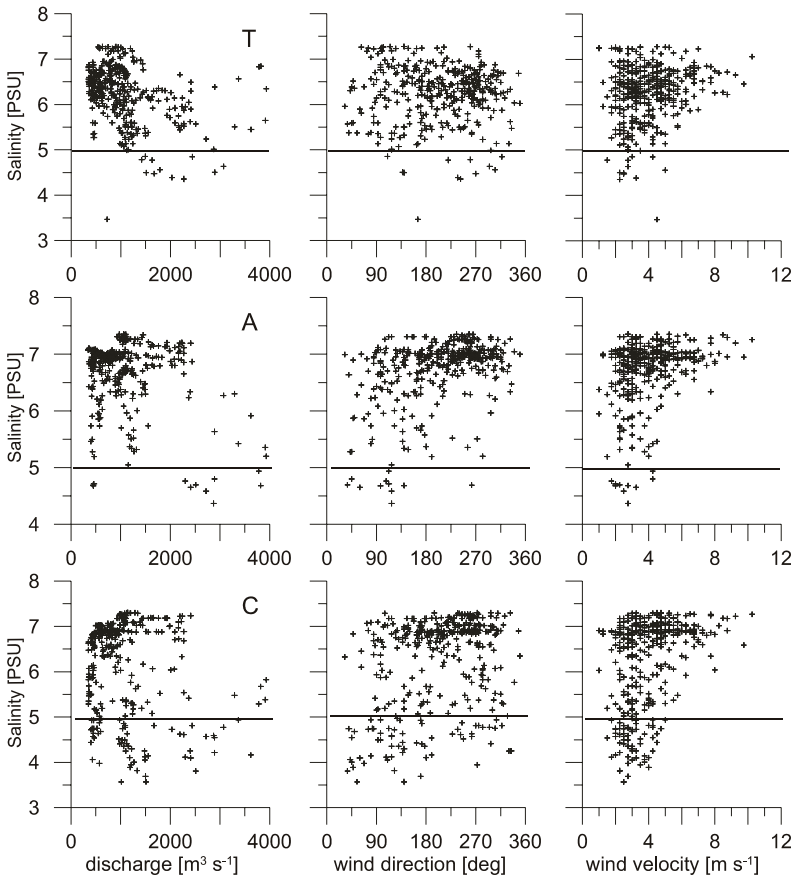


**Fig. 13.** Salinity at locations **T**, **A**, and **C** in relation to Vistula River discharge, wind direction and speed in 1994.

## CONCLUSIONS AND REMARKS

Hydrodynamic modelling enabled the reproduction of salinity, temperature and flow changes in 1994 in the Gulf of Gdańsk. The hydrological and meteorological conditions in the year analysed were fairly typical, without any extreme conditions. Wind conditions, as measured at the Hel station, were slightly milder than those averaged from past decades (1951-1975). As in past years westerly winds predominated in 1994.

Surface water currents, calculated by the model, confirmed that water movement in the Vistula Estuary is predominantly eastward (especially in the eastern part of the Estuary), in agreement with the prevailing wind direction.

Using salinity as a tracer of fluvial waters in the marine environment, it was found that the Vistula River water more frequently spread over larger distances (c.a. 20 km) to the west than the east, opposing the dominant direction of flow in that region. This phenomenon can be explained by high current speeds in an easterly direction and, in consequence, intensified vertical mixing processes.

The model results confirm earlier *in situ* observations of sporadic occurrences of fluvial water in the vicinity of the Hel Peninsula. It was found that such episodes are observed only where gentle east/southeast winds (below  $5 \text{ m s}^{-1}$ ) coincide with a river discharge exceeding approx.  $2000 \text{ m}^3 \text{ s}^{-1}$ .

## REFERENCES

- Eckart C. (1958). Properties of water. Part II. The equation of state of water and sea water at low temperatures and pressures. *Am. J. Sci.*, 256, 225-240.
- Fal B., Bogdanowicz E., Czernuszenko W., Bobrzyńska I. & Koczyńska A. (1997). *Przepływy charakterystyczne głównych rzek polskich w latach 1951-1990*. Seria Hydrologia i Oceanologia, 21, Warszawa: Instytut Meteorologii i Gospodarki Wodnej.
- Kwiatkowski J., Rasmussen E. K., Ezhova E. & Chubarenko B. (1997). The eutrophication model of the Vistula Lagoon, *Oceanol. Stud.*, 26(1), 5-33.
- Kwiecień K. (1990). Klimat. In: A. Majewski (Ed.), *Zatoka Gdańsk* (pp. 66-119). Warszawa: Wydawnictwa Geologiczne.
- Majewski A. & Bogacka T. (1983). *Charakterystyka hydrologiczna przedpola ujścia Wisły ze szczególnym uwzględnieniem cyrkulacji wód i wynoszenia zanieczyszczeń wodami Wisły, Opracowanie badań rejsowych za okres 1980-82*. Gdynia: Instytut Meteorologii i Gospodarki Wodnej.
- Nowacki J. & Matciak M. (1996). Warunki hydrologiczne w strefie frontu wód Wisły. *Przegląd Geofizyczny*, 41(4), 275-285.
- Nowacki J. & Matciak M. (2000). Characteristics of the selected hydrological parameters of the Gulf of Gdańsk in the planned area of sewage discharge from the "Gdańsk-Wschód" sewage-treatment plant. *Oceanol. Stud.*, 29(4), 83-98.
- Phillips N.A. (1957). A coordinate system having some special advantages for numerical forecasting. *J. Meteorol.*, 14(2), 184-185.
- Robakiewicz M. (1997). Hydrodynamic conditions in the Gulf of Gdańsk during POLRODEX'96 experiment in comparison with numerical model. *Oceanol. Stud.*, 26(4), 145-159.

- Robakiewicz M. (2000). Verification of a hydrodynamic model by statistical measures – example of Gdańsk Bay, In Fourth International Conference on Hydroinformatics, 23-27 July 2000 (CD-9 pages). Iowa Institute of Hydraulic Research: International Association of Hydraulic Research.
- Robakiewicz M. (2004). *Wybrane problemy matematycznego modelowania hydrodynamiki Zatoki Gdańskiej Problemy Modelowania*. Gdańsk, Instytut Budownictwa Wodnego PAN.
- WL|Delft Hydraulics (2006). Delft3D-FLOW [computer software]. Delft: WL | Delft Hydraulics.